Optical pH Measurements with Water Dispersion of Polyaniline Nanoparticles and Their Redox Sensitivity

ARTICLE *in* ANALYTICAL CHEMISTRY · JUNE 2006

Impact Factor: 5.64 · DOI: 10.1021/ac052252u · Source: PubMed

3 AUTHORS:

Tom Lindfors
Åbo Akademi University
64 PUBLICATIONS **1,304** CITATIONS
SEE PROFILE

Leo Harju
Åbo Akademi University
65 PUBLICATIONS **563** CITATIONS
SEE PROFILE

Ari Ivaska
Åbo Akademi University
318 PUBLICATIONS **9,570** CITATIONS
SEE PROFILE

Anal. Chem. **2006,** *78,* 3019−3026

Optical pH Measurements with Water Dispersion of Polyaniline Nanoparticles and Their Redox Sensitivity

Tom Lindfors,* Leo Harju, and Ari Ivaska

Process Chemistry Centre, c/o Laboratory of Analytical Chemistry, Åbo Akademi University, Biskopsgatan 8, 20500 Åbo/Turku, Finland

A new method for optical pH and redox measurements with a commercially available water dispersion of polyaniline (PANI) nanoparticles (mean particle size, 46 nm) is presented. The pH measurements are based on the acid−base equilibrium of PANI and were carried out either by combining both the automated sequential injection analysis (SIA) and UV−visible spectrophotometric techniques or with a fiber-optic light guide. In the former case, the detection was done in continuous mode at λ = 800 nm by using the SIA technique for transporting the sample to a flow-through cell, which was placed in the light path of the photometer. With the fiber-optic light guide, the detection was done in batch mode at λ = 400 and 580 nm. In both methods, fresh pH reagent (PANI) solution was used in each measurement, thus overcoming the problem with hysteresis (memory effect), which is usually observed with PANI films. The PANI nanoparticles were characterized with UV−visible spectroscopy in pH buffer solutions between pH 2−12 and a protonation constant of log$K_{H_{0.5}L}^{0.5H,L}$ = 4.4 was calculated from these data. Fast pH measurements can be done between pH 6 and 10.5 depending on the measuring technique. It is possible to determine pH with an accuracy of 0.1 pH unit between pH 8 and 10.5 (RSD, 0.5−2%). Redox transitions typical for PANI films were also observed for water solutions of PANI nanoparticles in the presence of the hexacyanoferrate(II/III) and the iron(II/III) oxalate redox couples. The absorbance at λ = 875 nm is linearly dependent on the logarithm of the concentration ratio (0.1−10) of the iron oxalate redox couple.

Polyaniline (PANI) is the most studied electrically conducting polymer (CP)[1] and was already reported as "aniline black" in 1862 by Letheby.[2] It has been studied extensively since the rediscovery of CPs in the late 1970s.[3] The preparation procedure of PANI has mainly been focused on electrochemical and different chemical polymerization methods usually resulting in insoluble and non-processable films and powders.[1] The processability and solubility in common organic solvents can, however, be improved by treating PANI with organic acids, e.g., camphorsulfonic acid, dodecylbenzenesulfonic acid, and phosphoric acid diesters,[4] or by functionalizing the polymer backbone with alkyl groups.[1] The solubility of PANI in organic solvents has been utilized, for example, in the construction of different types of all-solid-state ion-selective electrodes (ISEs), where PANI functions as the ion-to-electron transducer.[5−9] The insolubility of PANI in aqueous solutions were recently overcome when Wessling et al. reported a reproducible method for melt dispersion processing of PANI without solvents or secondary dopants.[10] It is now established that PANI can be reproducibly dispersed in water and different organic solvents by using appropriate counterions.[11,12] Different types of dispersions are today commercially available from Ormecon GmbH and Panipol Ltd.[13,14]

It is also well established that PANI is both pH[1,15] and redox sensitive.[16] For example, the oxidation state of a PANI film can be transformed in acidic solutions between the fully reduced insulating leucoemeraldine base (LEB), half-oxidized electrically conducting emeraldine salt (ES), and the fully oxidized insulating pernigraniline base (PNB) forms by varying the potential that is applied to the film (Figure 1a). The strong pH sensitivity of PANI, on the other hand, has been used for constructing different types of potentiometric[15,17−20] and optical[21−27] pH probes. In both cases,

* Corresponding author. E-mail: Tom.Lindfors@abo.fi. Fax: +358-2-2154479.

(1) Wallace, G. G.; Spinks, G. M.; Kane-Maguire, L. A. P.; Teasdale, P. R. *Conductive Electroactive Polymers: Intelligent materials systems,* 2nd ed.; CRC Press: Boca Raton, FL, 2003; pp 121−177.
(2) Letheby, H. *J. Chem. Soc.* **1862**, *15*, 161−163.
(3) Shirakawa, H.; Louis, E.; MacDiarmid, A. G.; Chiang, C. K.; Heeger, A. J. *J. Chem. Soc., Chem. Commun*. **1977**, *16*, 578−580.
(4) Pron, A.; Österholm, J.-E.; Smith, P.; Heeger, A. J.; Laska, J.; Zagorska, M. *Synth. Met.* **1993**, *57*, 3520−3525.
(5) Bobacka, J.; Lindfors, T.; McCarrick, M.; Ivaska, A.; Lewenstam, A. *Anal. Chem.* **1995**, *67*, 3819−3823.
(6) Sjöberg, P.; Lindfors, T.; Bobacka, J.; Lewenstam, A.; Ivaska, A. *Anal. Chim. Acta* **1999**, *385*, 163−173.
(7) Lindfors, T.; Ivaska, A. *Anal. Chim. Acta* **2000**, *404*, 111−119.
(8) Lindfors, T.; Ivaska, A. *Anal. Chim. Acta* **2001**, *437*, 171−182.
(9) Lindfors, T.; Ivaska, A. *Anal. Chem.* **2004**, *76*, 4387−4394.
(10) Wessling, B.; Srinivasan, D.; Rangarajan, G.; Mietzner, T.; Lennartz, W. *Eur. Phys. J. E* **2000**, *2*, 207−210.
(11) Wessling, B. *Synth. Met.* **2003**, *135−136*, 265−267.
(12) Kahol, P. K.; Ho, J. C.; Chen, Y. Y.; Wang, C. R.; Neeleshwar, S.; Tsai, C. B.; Wessling, B. *Synth. Met.* **2005**, *151*, 65−72.
(13) www.zipperling.de.
(14) www.panipol.com.
(15) Lindfors, T.; Ivaska, A. *J. Electroanal. Chem.* **2002**, *531*, 43−52.
(16) Genies, E. M.; Tsintavis, C. *Electroanal. Chem.* **1985**, *195*, 109−128.
(17) Karyakin, A. A.; Bobrova, O. A.; Lukachova, L. V.; Karyakina, E. E. *Sens. Actuators, B* **1996**, *33*, 34−38.
(18) Lindino, C. A.; Bulhões, L. O. S. *Anal. Chim. Acta* **1996**, *334*, 317−322.
(19) Cui, G.; Lee, J. S.; Kim, S. J.; Nam, H.; Cha, G. S.; Kim, H. D. *Analyst* **1998**, *123*, 1855−1859.

10.1021/ac052252u CCC: $33.50
Published on Web 03/28/2006

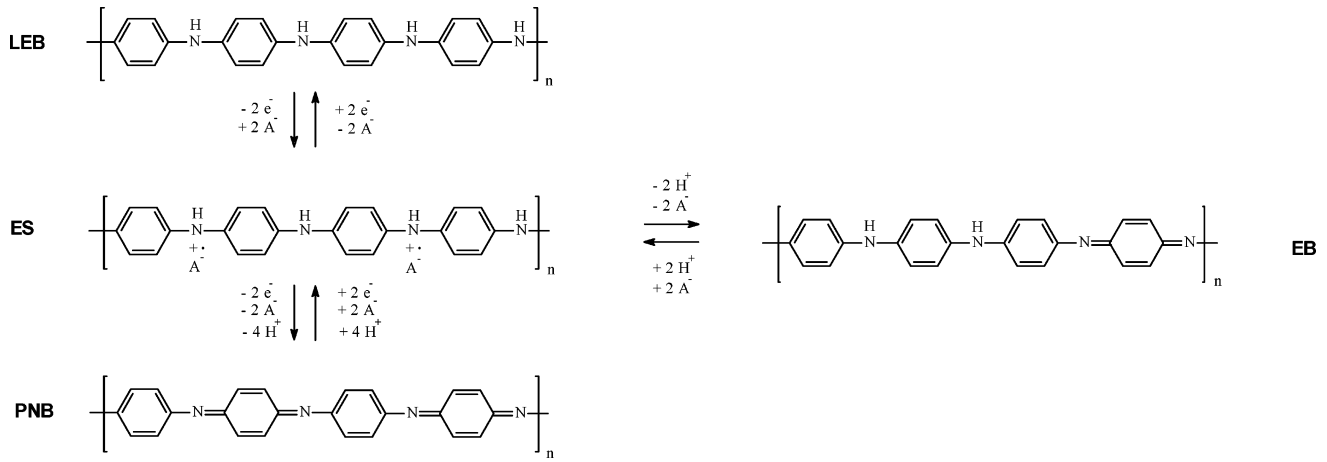

Figure 1. Redox mechanism between the LEB, ES, and PNB forms of PANI and the acid−base equilibrium between the ES and EB forms.

the acid−base equilibrium must be established between the emeraldine base (EB) and ES forms in the entire bulk of the PANI film (Figure 1), in contrast to many conventional poly(vinyl chloride) (PVC)-based ISEs where only minor time-dependent changes in the membrane bulk composition take place during the potentiometric measurement.[28,29] The thickness and composition of the PANI film determine how quickly the EB−ES equilibrium is established[15,30,31]. In some cases, the pH-dependent EB−ES transition can be strongly retarded by incorporating lipophilic anions to the PANI film.[31]

Also in bulk optodes, the equilibrium must be reached within the entire membrane (thickness ~1−2 μm) before measurements can be conducted.[28] Response times in the order of seconds have been obtained for relatively high analyte concentrations,[32] but the response time increases even to hours in strongly diluted solutions.[33] Bakker et al. have studied bulk optodes prepared with different neutral hydrogen-selective chromoionophores.[34] The measuring range of bulk optodes is usually 2−4 pH units, but it has been proposed that a much larger activity range than for conventional ISEs could be obtained with optical sensor arrays consisting of several optodes.[28] Bulk optodes have, however, some drawbacks. The response may be affected by, for example, changes in the optical properties of thicker optode membranes (water droplet formation resulting in turbidity), leaching of the active components from the membrane to the solution phase, and changes in the ion activities in the optode membrane.[28] The response mechanism of bulk optodes is also more complex than for conventional ISEs because a coextractant must be incorporated in the membrane. Phase-transfer equilibrium must therefore be established between two ions in the optode membranes, and consequently, bulk optodes cannot be sensitive only for one specific ion.

In this paper, a new, simple, and fast photometric method to measure pH with water dispersion of PANI nanoparticles is presented. The pH measurement is done in continuous mode by combining both the automated sequential injection analysis (SIA) system[35,36] and UV−visible spectroscopy or by measuring pH in batch mode using only a fiber-optic light guide. The acid−base equilibrium of the PANI nanoparticles is established entirely in the solution phase. The hysteresis effect, which is usually observed in pH measurements with PANI films,[15] should thus be avoided because a fresh PANI solution is used in each measurement. The PANI nanoparticles have a mean particle size of only 46 nm, and the acid−base equilibrium is therefore also established faster in the nanoparticles than in the much thicker PANI and bulk optode films with film thicknesses of at least several hundreds of nanometers or more. We have also studied whether the same redox chemistry as for solid PANI films is valid for PANI nanoparticles in the solution phase.

EXPERIMENTAL SECTION

Chemicals. (a) PANI Water Dispersion. The PANI water dispersion (D1012W-1) (mean particle size: 46 nm; pH 1.4) was obtained from Ormecon GmbH (Ammersbek, Germany). The size of 90% of the particles was <66 nm, and the conductivity in a vacuum was given as 0.44 S/cm (spin-coated PANI films on ITO/glass substrate). The PANI water dispersion contains poly(styrenesulfonic acid) (PSSA) as dopant with two sulfonate groups per a two-ring unit of PANI.[12] The PSSA groups are located in a disordered region surrounding the ordered ("metallic") inner core

(20) Karyakin, A. A.; Vuki, M.; Lukachova, L. V.; Karyakina, E. E.; Orlov, A. V.; Karpachova, G. P.; Wang, J. *Anal. Chem.* **1999**, *71*, 2534−2540.
(21) Ge, Z.; Brown, C. W.; Sun, L.; Yang, S. C. *Anal. Chem.* **1993**, *65*, 5, 2335−2338.
(22) Pringsheim, E.; Terpetschnig, E.; Wolfbeis, O. S. *Anal. Chim. Acta* **1997**, *357*, 247−252.
(23) Grummt, U.-W.; Prón, A.; Zagorska, M.; Lefrant, S. *Anal. Chim. Acta* **1997**, *357*, 253−259.
(24) de Marcos, S.; Asensio, C.; Uruñuela, I.; Gallarta, F.; Galbán, J.; Castillo, J. R. *Quim. Anal.* **2000**, *19 (Suppl 1)*, 99−104.
(25) Jin, Z.; Su, Y.; Duan, Y. *Sens. Actuators, B* **2000**, *71*, 118−122.
(26) Pandey, P. C.; Singh, G. *Talanta* **2001**, *55*, 773−782.
(27) Lindfors, T.; Ivaska, A. *J. Electroanal. Chem.* **2005**, *580*, 320−329.
(28) Bakker, E.; Bühlmann, P.; Pretsch, E. *Chem. Rev.* **1997**, *97*, 3083−3132.
(29) Sokalski, T.; Lingenfelter, P.; Lewenstam, A. *J. Phys. Chem. B* **2003**, *107*, 2443−2452.
(30) Lindfors, T.; Ivaska, A. *J. Electroanal. Chem.* **2002**, *535*, 65−74.
(31) Lindfors, T.; Sandberg, H.; Ivaska, A. *Synth. Met.* **2004**, *142*, 231−242.
(32) Morf, W. E.; Seiler, K.; Rusterholz, B.; Simon, W. *Anal. Chem.* **1990**, *62*, 738−742.
(33) Lerchi, M.; Reitter, E.; Simon, W.; Pretsch, E.; Chowdhury, D. A.; Kamata, S. *Anal. Chem.* **1990**, *66*, 1713−1717.
(34) Bakker, E.; Lerchi, M.; Rosatzin, T.; Rusterholz, B.; Simon, W. *Anal. Chim. Acta* **1993**, *278*, 211−225.
(35) Růžička, J.; Marshall, G. D. *Anal. Chim. Acta* **1990**, *237*, 329−343.
(36) Kullberg, N.; Vilén, M.; Sund, P.; Talaslahti, M.; Sara, R. *Talanta* **1999**, *49*, 961−968.

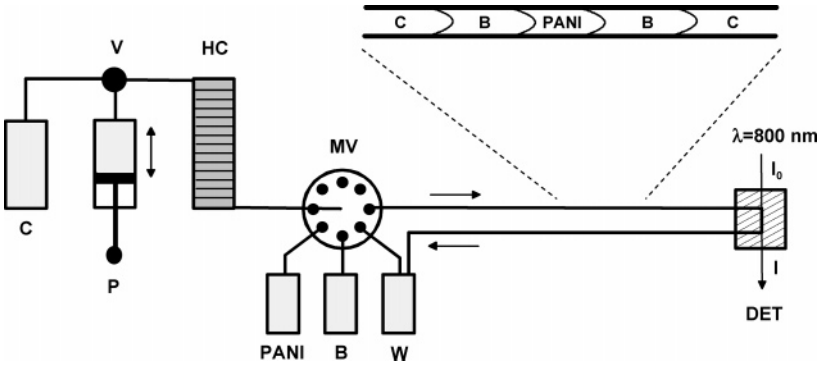

Figure 2. Experimental setup of the combined SIA and UV−visible measurements. Key: C, carrier solution (deionized water); P, piston pump; V, valve; HC, holding coil; MV, multiport valve; PANI, PANI water dispersion (1:100); B, pH buffer solution (pH 2−12); W, waste; DET, UV−visible detector operating at $\lambda = 800$ nm.

of the nanoparticles (size, ~10 nm). The D1012W-1 dispersion was stored in a closed bottle, and diluted solutions were prepared from this stock solution by dilution with deionized water ($R \geq 18.2$ MΩ).

(b) pH Buffer Solutions. The pH buffer solutions used in this study were prepared according to Perrin and Dempsey[37] and consisted of 25 mM citric acid (monohydrate) (≥99.5%), 25 mM Tris (p.a. ≥99.8%), 25 mM KCl (p.a. ≥99.5%)—obtained from Fluka—25 mM KH_2PO_4 and 25 mM $NaB_4O_7 \cdot 10H_2O$ (Merck). The pH buffer solutions were prepared with deionized water ($R \geq 18.2$ MΩ), and pH was adjusted with HCl or NaOH. Separate buffer solutions were prepared for each pH covering the pH range from 2 to 12.

(c) Redox Buffer Solutions. The redox measurements were done in 10 mM hexacyanoferrate(II/III) ($Fe(CN)_6^{3-/4-}$; $E° = 0.69$ V vs NHE) and 10 mM iron(II/II) oxalate ($Fe(C_2O_4)_3^{3-/4-}$; $E° = -0.20$ V vs NHE) redox solutions with [ox]/[red] ratio varying between 0.01 and 100. The redox solutions were buffered to pH 6 with 40 mM phosphate buffer in order to eliminate possible interferences from the pH dependent EB−ES equilibrium (Figure 1). The iron oxalate redox solutions were prepared by adding 0.5 mL of a 50 mM solution of $FeCl_2$ and $FeCl_3$, with [ox]/[red] = 0.01−100, to 2 mL of a 50 mM phosphate buffer solution containing 1.25 M potassium oxalate.[38] Both oxalate and cyanide are more strongly bound to Fe^{2+} and Fe^{3+} than phosphate, and thus, phosphate buffer solutions can be used in the redox measurements without affecting the [ox]/[red] ratio of the redox couples. $K_4Fe(CN)_6$, $K_3Fe(CN)_6$, KH_2PO_4, K_2HPO_4, $K_2C_2O_4$, $FeCl_2$, and $FeCl_3$ were obtained from Merck.

UV−Visible Measurements. (a) Measurements with the Double-Beam Spectrophotometer. The pH sensitivity of the PANI nanoparticles was determined in pH buffer solutions with pH 2−12. UV−visible spectra were measured between 325 and 1100 nm by adding 50 μL of dispersion (volume ratio of D1012W-1 stock solution to deionized water, 1:9) to 2 mL of pH buffer solution. The UV−visible spectrum was recorded either after an equilibration time of 10 (pH 2−12) or 30 min (pH 7−10). The background spectrum was always recorded for each buffer solution by filling both the sample and reference cuvettes with 2 mL of pH buffer solution. The pH buffer solutions absorb practically no light (like deionized water) in the wavelength region given above. The cuvettes were always closed with plastic caps before starting the measurements to avoid evaporation of the solution.

The photometric redox sensitivity of the PANI nanoparticles was determined in redox solutions with [ox]/[red] = 0.01−100. The 50-μL PANI dispersion (1:9) was added to 2.5 mL of the redox solutions described above. The UV−visible spectra (325−1100 nm) were measured with 2-min intervals during 18 min. The background spectrum was always recorded in 40 mM phosphate buffer solution containing either 10 mM hexacyanoferrate(II/III) or 10 mM iron(II/III) oxalate (in potassium oxalate) before the measurements were started. All UV−visible spectra were recorded with a Hitachi U-2001 spectrophotometer at 23 ± 1 °C. The cuvettes were always closed with plastic caps before the measurements were started to avoid evaporation of the solution.

(b) Measurements with the Fiber-Optic Light Guide. The UV−visible measurements with the fiber-optic light guide, which was connected to a Metrohm 662 photometer (wavelength range, $\lambda = 400-700$ nm), were done either at $\lambda = 400$ nm or $\lambda = 580$ nm by adding 200 (measurements at 400 nm) or 250 μL (at 580 nm) of the PANI water dispersion (1:9) to 10 mL of pH buffer solution (pH 2−12). The incoming light from one of the fiber-optic light guide halves passes through the sample solution to the reflector (concave mirror), which is attached to the stainless steel body of the light guide. The light beam is then reflected back through the solution to the other half of the optical fiber, resulting in a total light path length of ~2 cm. The absorbance was measured for 5 min after the addition of PANI to the solution and was set to zero in each pH buffer solution before starting the measurements.

Combined SIA and UV−Visible Measurements. The experimental setup of the combined SIA and UV−visible measurements is schematically shown in Figure 2. A commercial SIAmate analyzer from Arctic Instruments Oy Ab (Turku, Finland) was used in the flow measurements.[36] A plug of 400 μL of pH buffer solution (B) was first transferred with the piston pump (P, flow rate, 50 μL/s) to the holding coil (HC, tube diameter, 1 mm) via the multiport valve (MV), followed by 80 or 100 μL of PANI water dispersion (1:100; 20 μL/s) and 400 μL of pH buffer solution (50 μL/s). Deionized water was used as carrier solution (C). The

(37) Perrin, D. D.; Dempsey, B. *Buffers for pH and Metal Ion Control*; Chapman and Hall: London, 1974; p 48.
(38) Kolthoff, I. M.; Lingane, J. J. *Polarography*, 2nd ed.; Interscience Publishers: New York, 1952; Vol. 1, p 219.

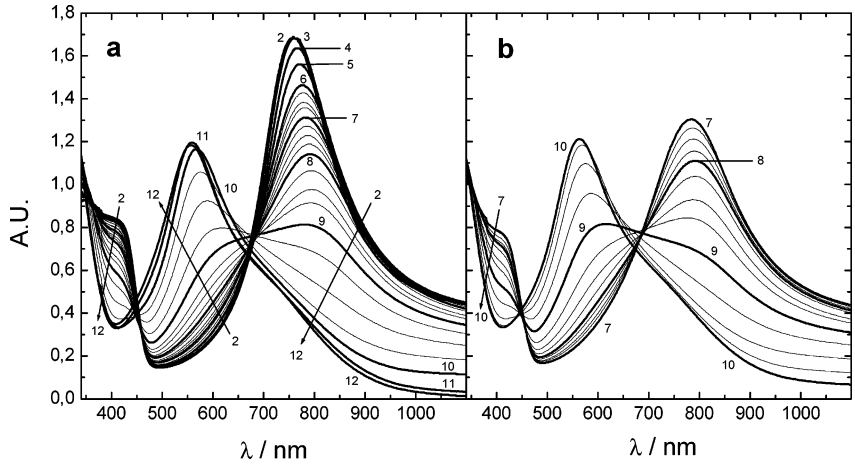

Figure 3. UV−visible spectra of the PANI water dispersion (D1012W-1; 1:9) in pH buffer solutions. (a) pH 2−12, equilibration time: 10 min. (b) pH 7−10, equilibration time: 30 min. The UV−visible spectra were measured with ΔpH = 0.25 between pH 6 and 10.

pump direction was then reversed and the C−B−PANI−B−C plug was reproducibly transported with a flow rate of 120 μL/s to the flow-through cell (Hellma 178.710-QS cell, $d = 3$ mm; optical path length, 10 mm) and the light path of the detector (DET) operating at $\lambda = 800$ nm. The UV−visible spectra of the PANI nanoparticles show considerable pH-dependent changes at 800 nm resulting in a large measuring range (Figure 3). The tube diameter and tube length between the multiport valve and detector was 1 mm and ∼55 cm, respectively. Disturbances in the UV−visible detector response were caused by stray light that was transferred to the flow-through cell via Teflon tubings connected to the inlet and outlet of the cell. The tubings were therefore covered with black outer tubings in order to eliminate these disturbances.

The Teflon tubings also serve as a reaction chamber for the pH buffer solution and PANI plugs. In general, the contact time between the pH buffer solution and PANI can be controlled by the flow rate and the UV−visible signal can therefore be recorded at different degrees of non-steady-state equilibrium or at equilibrium. The dispersion rate can also be changed by varying the inner diameter of the tubing. The tubings of the pH buffer and PANI ports (MV) were washed with 3 × 300 μL of pH buffer solution and 2 × 500 μL of PANI water dispersion, respectively, before the measuring sequence with buffers from low to high pH was started. Five measurements ($n = 5$) were done at each pH, and the tubing of the pH buffer port was always washed with the new buffer solution (3 × 300 μL) when the pH buffer solution was changed. The detector was washed with 2 mL of the carrier solution (100 μL/s) after each pH measurement. A tightly closed quartz cuvette filled with deionized water was placed in the reference light path, and the absorbance was automatically set to zero by the photometer before each measurement was started. The absorbance of the pH buffer solutions and water at $\lambda = 800$ nm were the same, i.e., practically zero. The total time of one pH measurement was ∼60 s but can be made shorter by optimizing the experimental procedure.

RESULTS AND DISCUSSION

Characterization of the EB−ES Transition. The UV−visible spectra of the PANI water dispersion, which were measured after an equilibration time of 10 (pH 2−12) and 30 min (pH 7−10), are shown in Figure 3a and b. The spectra were measured with pH intervals of ΔpH = 0.25 between pH 6 and 10. Only very small time-dependent changes were observed in the UV−visible spectra between pH 2 and ∼8.5, whereas more pronounced time-dependent changes were observed between pH 8.75 and 9.75. It can therefore be expected that the EB−ES transition mainly takes place in this pH interval. The UV−visible spectrum recorded at pH 2 is typical of the electrically conducting ES form of PANI with characteristic absorbance maximums at ∼415 and 757 nm associated with polaron band transitions (Figure 3a).[39] The rather narrow band with a peak at 757 nm indicates a localized charge distribution in the PANI nanoparticles.[40] On the other hand, the nonconducting EB form has a characteristic absorbance maximum at 568 nm (pH 10).[31,41] The spectra measured between pH 2 and 9 show two rather well-defined isosbestic points at ∼450 and ∼685 nm indicating that the ES form is transformed directly to the EB form. Deviations from the isosbestic points were, however, observed at higher pH values. It should also be noted that the color of the PANI solution became dark blue-violet at pH 11 and 12 (dark blue at pH 10), indicating the presence of a small amount of PNB impurities (violet) in the PANI water dispersion. It can be concluded based on the UV−visible measurements that the ES−EB transition of the PANI water dispersion takes place between pH 6 and 10 and the most pronounced changes in the absorbance spectra are observed at ∼400−420, ∼530−600, and ∼750−840 nm.

Determination of the Protonation Constant of PANI. The protonation constant (equilibrium constant of the protonation reaction) of the PANI water dispersion was calculated with data obtained from the UV−visible spectra measured between pH 6 and 10 (Figure 3a and b). The following general reaction stoichiometry was considered between the proton and the EB form (L) when calculating the protonation constant ($K^{n\mathrm{H,L}}_{\mathrm{H}_n\mathrm{L}}$) according to the definition used by Sillén and Martell:[42]

$$n\mathrm{H}^+ + \mathrm{L} \rightleftharpoons \mathrm{H}_n\mathrm{L}^{n+} \quad (1)$$

$$K^{n\mathrm{H,L}}_{\mathrm{H}_n\mathrm{L}} = [\mathrm{H}_n\mathrm{L}^{n+}]/[\mathrm{H}^+]^n[\mathrm{L}] \quad (2)$$

where n is the average proton number of the reaction.

(39) Laska, J.; Trznadel, M.; Prón, A. *Mater. Sci. Forum* **1993**, *122*, 177−184.

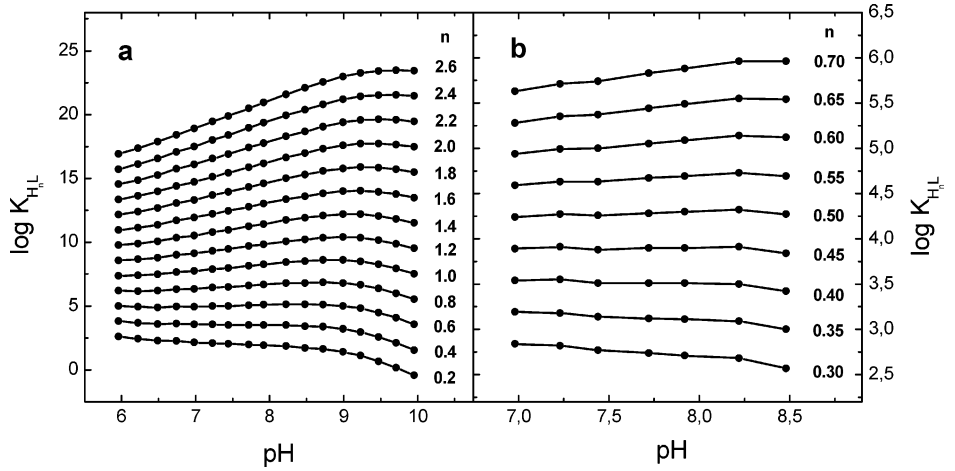

Figure 4. Protonation constants (log $K^{n\mathrm{H,L}}_{\mathrm{H}_n\mathrm{L}}$) of the PANI water dispersion (D1012W-1) calculated for different reaction stoichiometries (eq 1) with (a) $n = 0.2-2.6$ and (b) $n = 0.3-0.7$.

The protonation constant was calculated from data obtained at 400 and 800 nm. At these wavelengths, the absorbance of the H_nL^{n+} form (ES form) is higher than for L (Figure 3), which was considered in the derivation of the equation for determination of the protonation constant. Different methods have been proposed for the calculation of stability constants from spectrophotometric data.[43−45] The expression for the protonation constant was derived according to Bishop[43] resulting in eq 3 (see Supporting Information for detailed derivation):

$$K^{n\mathrm{H,L}}_{\mathrm{H}_n\mathrm{L}} = \frac{1}{[\mathrm{H}^+]^n}\frac{A - A_{\min}}{A_{\max} - A} \qquad (3)$$

The protonation constant was calculated with eq 3 from the absorbance (400 and 800 nm) and pH data by assuming different reaction stoichiometries with $n = 0.2-2.6$. As shown in Figure 4a, the calculated protonation constant is almost constant between pH 6 and 9 for $n = 0.4$ and 0.6. The protonation constant was therefore determined more accurately between pH 7.0 and 8.5 ($\mu \cong 0.2$) by varying n from 0.3 to 0.7 (Figure 4b). Two well-defined isosbestic points and no significant time-dependent changes of the UV−visible spectra were observed in this pH interval. It can be concluded based on the results shown in Figure 4b and Table 1 that the reaction stoichiometry is best described by $n = 0.5$ (minimum of the standard deviations at $n = 0.48$) resulting in a mixed protonation constant of log $K^{0.5\mathrm{H,L}}_{\mathrm{H}_{0.5}\mathrm{L}} = 4.4$ (mean value of the protonation constants given in Table 1 for $\lambda = 400$ and 800 nm). A mixed constant means by definition that the activity of hydrogen ions is used in the calculation of the protonation constant, whereas the concentrations are used for the other components.[46] As can be seen in Figure 1a, the EB to ES transition involves protonation of a four-ring unit of PANI by two hydrogen ions. This indicates that L in eq 1 is equal to one PhN unit when $n = 0.5$. Due to the excess of PSSA (two sulfonate groups per two-ring unit of PANI[12]), the degree of protonation of the ES form could not be exactly determined by photometric titration of the PANI water dispersion with diluted NaOH. The degree of protonation of PANI will be studied in more detail in a separate paper.

Table 1. Logarithmic Protonation Constants of the PANI Water Dispersion (D1012W-1)[a]

$\lambda = 400$ nm			$\lambda = 800$ nm		
n	log$K^{n\mathrm{H,L}}_{\mathrm{H}_n\mathrm{L}}$	SD[b]	n	log$K^{n\mathrm{H,L}}_{\mathrm{H}_n\mathrm{L}}$	SD[b]
0.30	2.97	0.102	0.30	2.73	0.092
0.35	3.35	0.108	0.35	3.12	0.066
0.40	3.74	0.055	0.40	3.50	0.041
0.45	4.12	0.037	0.45	3.89	0.022
0.50	4.51	0.035	0.50	4.28	0.027
0.55	4.90	0.050	0.55	4.66	0.049
0.60	5.28	0.073	0.60	5.05	0.074
0.65	5.67	0.097	0.65	5.43	0.100
0.70	6.05	0.123	0.70	5.82	0.127

[a] The constants given are mean values of logarithmic protonation constants calculated in the pH interval of 7.0−8.5 (Figure 4b) from data obtained from UV−visible spectra at $\lambda = 400$ and 800 nm (Figure 3b). The following stoichiometry was used in the calculations: $n\mathrm{H}^+ + \mathrm{L} \rightleftharpoons \mathrm{H}_n\mathrm{L}^{n+}$, where L and $\mathrm{H}_n\mathrm{L}^{n+}$ are the EB and ES forms of PANI, respectively. [b] Standard deviation.

Determination of the protonation constant of PANI is of great importance for many practical applications, e.g., in ion sensors. For instance, in certain applications, high pH sensitivity is desirable, whereas the pH sensitivity must be suppressed in other applications. It was recently shown that the pH sensitivity of PANI could be strongly suppressed by incorporating lipophilic anions in the PANI membrane.[31] The protonation constants of different types of PANIs provide direct information about the pH sensitivity of the materials and can therefore be used in theoretical considerations when choosing the right PANI material for a specific application.

(40) Xia, Y. In *Electrical and Optical Polymer Systems; Fundamentals, Methods and Applications*; Wise, D. L., Wnek, G. E., Trantolo, D. J., Cooper, T. M., Gresser, J. D., Eds.; Marcel Dekker: New York, 1998; p 366.
(41) McCall, R. P.; Ginder, J. M.; Leng, J. M.; Ye, H. J.; Manohar, S. K.; Masters, J. G.; Asturias, G. E.; MacDiarmid, A. G.; Epstein, A. J. *Phys. Rev. B* **1990**, *41*, 5202−5213.
(42) Sillén, L. G.; Martell, A. E. *Stability constants of metal-ion complexes*; Stability Constants No. 17; The Chemical Society: London, 1964.
(43) Bishop, E., Ed. *Indicators*; Pergamon Press: New York, 1972; pp 56−59.
(44) Ramette, R. W. *J. Chem. Educ.* **1967**, *44*, 647−654.
(45) Ingman, F. *Talanta* **1973**, *20*, 993−997.
(46) Ringbom, A. *Complexation in Analytical Chemistry*; Wiley-Interscience: New York; 1963; p 25.

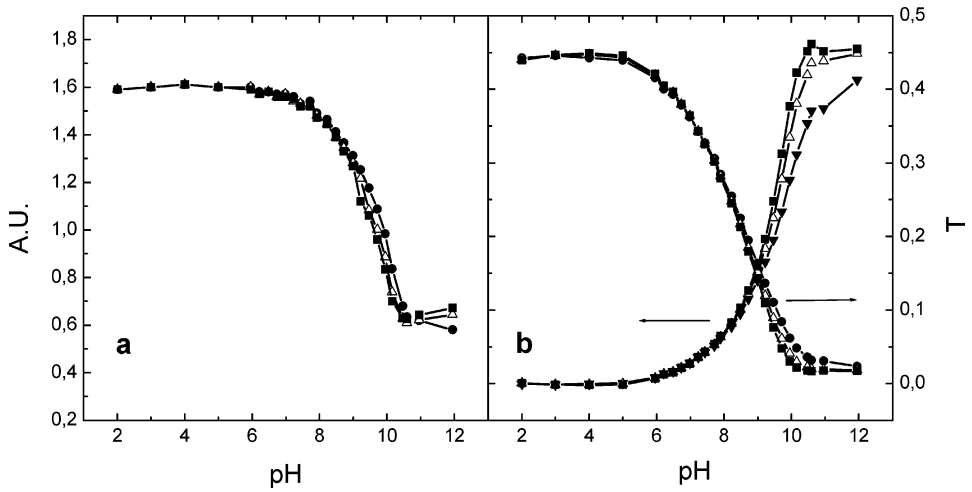

Figure 5. Absorbance as a function of pH at (a) $\lambda = 400$ nm and (b) $\lambda = 580$ nm for the fiber-optic light guide measured after an equilibration time of 30 s (●), 1 min (△), and 2 min (■). Transmittance versus pH is also shown in (b).

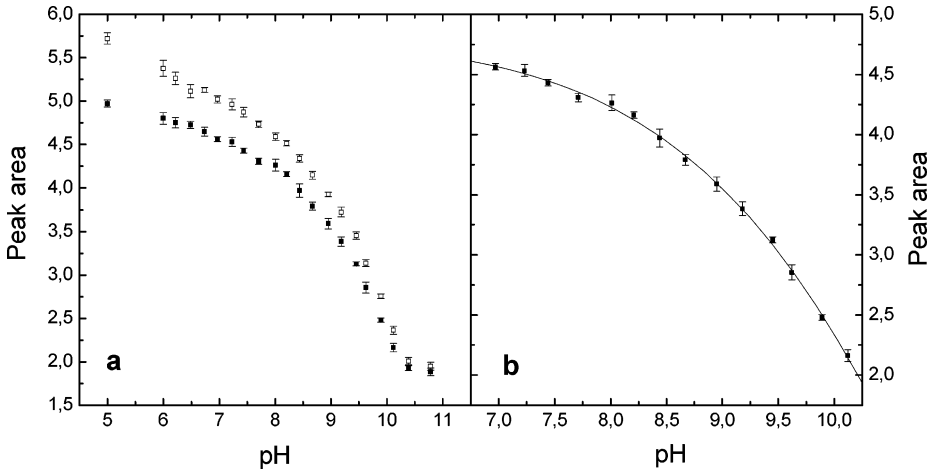

Figure 6. (a) Peak area as a function of pH for the C−B−80−B−C (■) and C−B−100−B−C (□) configuration in the combined SIA and UV−visible measurements. (b) The experimental data points of the C−B−80−B−C configuration are described between pH 7 and 10.1 by the third-order polynomial: $pH = 12.60 - 3.582PA + 0.563PA^2 - 0.031PA^3$ ($r^2 = 0.999$), where PA is the peak area.

pH Measurements with the Fiber-Optic Light Guide. The absorbance as a function of pH was measured with the fiber optical sensor at $\lambda = 400$ (Figure 5a) and 580 nm (Figure 5b). The EB−ES equilibrium is quickly established, and stable absorbance values with only minor time-dependent drifts were obtained in the pH interval between 2 and 8.5 already after 10 s (not shown in the figures) and especially after 30 s (Figure 5a). In both cases, more significant time-dependent drifts of the absorbance values were observed between pH 8.75 and 10.5, which is in good accordance with the time-dependent drifts shown in Figure 3 (compare the spectra in Figure 3a and b, which were measured at, for example, pH 9 after an equilibration time of 10 and 30 min, respectively). It is possible to determine pH with an accuracy of 0.1 pH unit between pH 8 and 10.5 at $\lambda = 400$ nm (Figure 5a) due to the high stability of the Metrohm 662 photometer. On the other hand, it can be more advantageous to use the transmittance mode for pH measurements at $\lambda = 580$ nm (Figure 5b). Also a broader pH range can be covered at this wavelength than at $\lambda = 400$ nm. At $\lambda = 580$ nm, pH can be determined with a precision of 0.2 pH unit between pH 6 and 7 and with 0.1 pH unit between pH 7 and 10. It should be noted that the transition interval of PANI (~4 pH units) is broader than for conventional acid−base indicators in general (two pH units; usually $pH = pK_{ind} \pm 1$) due to the stoichiometric factor of $n = 0.5$ for the protonation reaction of PANI. Another advantage of this simple optical batch method is that pH can be measured quickly with good precision and a rather small amount of reagent (PANI).

pH Measurements with the Flow-Through Cell. A simple automated analysis method combining the SIA and UV−visible techniques was developed in order to reduce the PANI and pH buffer solution volumes (Figure 2). The pH measurements were done with 80 or 100 μL of PANI solution at $\lambda = 800$ nm in order to obtain a large dynamic range. Two different SIA plug configurations were therefore used in the measurements: C−B−80−B−C or C−B−100−B−C. The results of the measurements are shown in Figure 6a. The best reproducibility is obtained when the area of the absorbance peak is plotted as a function of pH. Typical absorbance peaks for the C−B−80−B−C plug configuration are shown in Figure 7. It can be seen that the reproducibility of the absorbance maximum decreases at higher absorbances. This is probably due to the insufficient detector stability of the photometer when it is used in the flow-through configuration and can probably be overcome with a photometer more suitable for flow-through measurements. The reproducibility of the measurements shown

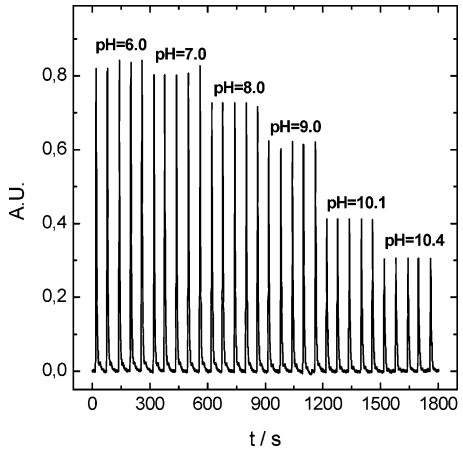

Figure 7. Typical absorbance peaks at pH 6.0, 7.0, 8.0, 9.0, 10.1, and 10.4 for the C−B−80−B−C configuration in the combined SIA and UV−visible measurements.

in Figure 6a is, however, still rather good with a relative standard deviation varying between 0.5 and 2% (n = 5). The measuring range is improved with the higher PANI volume (C−B−100−B−C) and by this configuration pH can be measured with a sensitivity of 0.2 pH unit between pH 7 and 8 and with 0.1 pH unit between pH 8 and 10.5.

In Figure 6b, pH is plotted as function of the peak area between pH 7 and 10.1 for the C−B−80−B−C configuration. The following third-order polynomial was fitted to these experimental values using Origin 7.5: $pH = 12.60 - 3.582PA + 0.563PA^2 - 0.031PA^3$ ($r^2 = 0.999$; PA, peak area). It is clear that a nonlinear relationship between pH and peak area is not as convenient in practical applications as a linear relationship. It is not, however, a limitation if proper standard buffer solutions, e.g., pH 7, 8, 9, and 10, are used in combination with proper software. The most important requirement for successful application of the method is the reproducibility of the pH measurements. This criterion is fulfilled with the SIA technique. Alternatively, pH can be determined by measuring only the mixed absorbance (A) when the protonation constant of PANI is known. This requires also a highly reproducible method resulting always in the same A_{min} and A_{max}.

Redox Measurements. The redox measurements were done in order to study whether the same redox chemistry as for solid PANI films (LEB−ES−PNB transitions) is also valid for the PANI nanoparticles in the solution phase. The UV−visible measurements show that it is possible to reduce the ES form of PANI almost completely to the LEB form (Figure 1) in the presence of a low [ox]/[red] ratio of the iron oxalate redox couple, which has a low standard potential (Figure 8a). The ES to LEB transition was confirmed by the color change from green (ES) to transparent/light yellow (LEB). It is, however, impossible to determine the exact color of the LEB form because the iron oxalate solution is light yellow. When the [ox]/[red] ratio is lowered, the absorbance maximum characteristic of the ES form at 415 nm decreases and finally disappears at the lowest [ox]/[red] ratio. The other absorbance maximum of the ES form at 830 nm ([ox]/[red] = 100) is simultaneously shifted to 904 nm ([ox]/[red] = 0.01), indicating that PANI is still partially in the ES form. The peak shift to higher wavelengths (lower energies) is typical for the ES to LEB transition and has been reported earlier for solid PANI films.[47] It should be pointed out that the LEB form does not have any absorbance maximums in the studied wavelength region.[47] The interferences observed in the spectra at λ <390 nm were caused by the iron oxalate redox couple.

The ES form of PANI was converted to the PNB form in contact with the hexacyanoferrate redox couple having a high redox potential (Figure 8b). The absorbance peak at 810 nm ([ox]/[red] = 0.01) is shifted to 614 nm ([ox]/[red] = 100) as the [ox]/[red] ratio of the redox couple increases. The color of the solution changes at the same time from green to violet. It is well known that the PNB form has an absorbance maximum at ~560 nm.[48] The absorbance maximum of the ES form at ~400 nm can still be observed in the spectra obtained in the presence of the redox couples with [ox]/[red] = 0.01−0.2, but at higher [ox]/[red] ratios, this maximum cannot be seen due interferences from $Fe(CN)_6^{3-}$. It can be concluded that the oxidation state of the PANI nanoparticles can be varied between the fully reduced LEB, half-oxidized ES, and fully oxidized PNB forms. The same redox chemistry as with solid PANI films can therefore be carried out with PANI nanoparticles in the solution phase.

A linear relationship between the absorbance of the PANI nanoparticles and the logarithm of the $[Fe(C_2O_4)_3^{3-}]/[Fe(C_2O_4)_3^{4-}]$ ratio was observed at 875 nm when the concentration

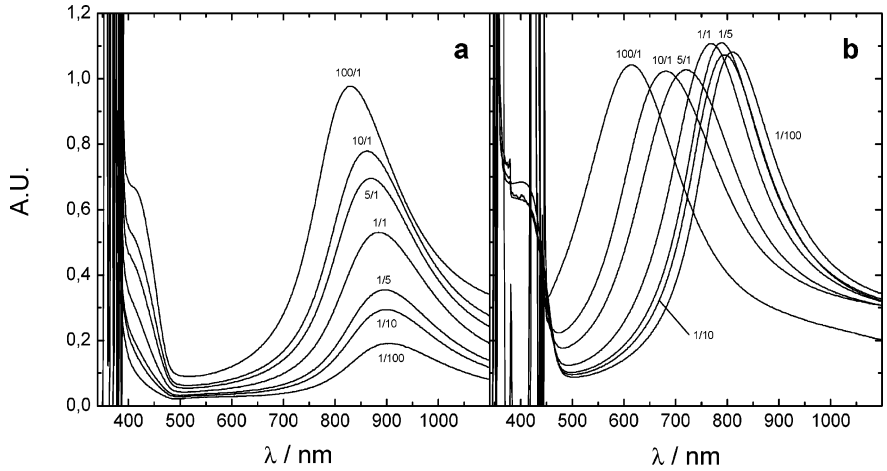

Figure 8. UV−visible spectra of the PANI water dispersion (D1012W-1; 1:9) measured in (a) 10 mM iron(II/III) oxalate and (b) 10 mM hexacyanoferrate(II/III) redox solutions after an equilibration time of 18 min. The measurements were done in a 40 mM phosphate buffer solution (pH 6) with [ox]/[red] = 0.01−100.

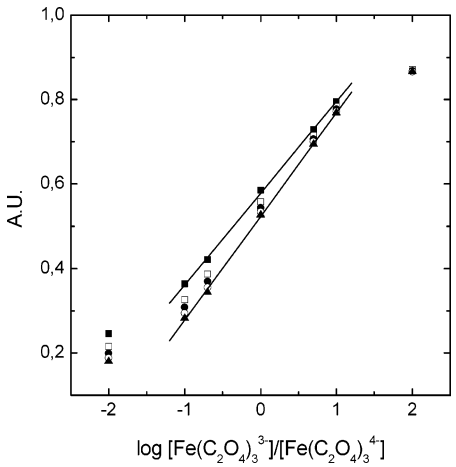

Figure 9. Absorbance of the PANI water dispersion (D1012W-1; 1:9) measured at $\lambda = 875$ nm in a 10 mM iron(II/III) oxalate redox solution after an equilibration time of 2 (■), 6 (□), 10 (●), 14 (○), and 18 min (▲). The measurements were done in a 40 mM phosphate buffer solution (pH 6) with [ox]/[red] = 0.01−100.

ratio was varied from 0.1 to 10. The time-dependent redox responses, which were measured after equilibration times of 2, 6, 10, 14, and 18 min, are shown in Figure 9. Highly linear relationships ($r^2 = 0.9995-0.9996$) were obtained for all equilibration times. The reason for the linear relationship was not studied in further detail.

CONCLUSIONS

A new optical method for pH measurements between pH 6 and 10.5 was developed in this work. The method combines the automated SIA and UV−visible techniques and is based on the acid−base equilibrium of a commercially available water dispersion of PANI nanoparticles with the mean particle size of 46 nm. Alternatively, pH can be measured in batch mode with a fiber-optic light guide. The pH measurements can be carried out with a good reproducibility and low reagent (PANI) consumption. Depending on the detection technique, pH can be determined with an accuracy of 0.2 pH unit between pH 7 and 8 and with 0.1 pH unit between pH 8 and 10.5.

The hysteresis effect that is usually observed in pH measurements with PANI films can be avoided with PANI nanoparticles because a fresh PANI solution is used for each measurement. The protonation equilibrium is also established faster in small nanoparticles than in films, which usually have a thickness of at least several hundreds of nanometers. It must be stressed that the protonation constants provide important information about the pH sensitivity of different types of polyanilines and can therefore be used when choosing right PANI materials for specific applications where either pH sensitivity or insensitivity is required. A protonation constant of $\log K^{0.5H,L}_{H0.5L} = 4.4$ ($n = 0.5$) was calculated for the PANI nanoparticles from data obtained from UV−visible measurements.

Possible application areas of the presented optical pH measurement methods are, for example, automated flow analysis systems where the application of the glass pH electrode is difficult, determination of pH under elevated pressures, and pH measurements of seawater where the sodium error may limit the use of the glass pH electrode. The limitations of absorbance measurements of real samples should, however, be considered when developing new optical methods.

The redox sensitivity of the PANI nanoparticles can, on the other hand, be used for determination of redox species at constant pH in water solutions. It was shown that the PANI nanoparticles dispersed in water solutions undergo the same redox chemistry as solid PANI films.

The chemical structure of the repeating unit of PANI is very similar to conventional acid−base and redox indicators, like indophenols, azo compounds, and variamine blues. It is therefore not surprising that the PANI nanoparticles can be used both as acid−base and redox indicators in water solutions.

(47) Quillard, S.; Berrada, K.; Louarn, G.; Lefrant, S.; Lapkowski, M.; Pron, A. *New J. Chem.* **1995**, *19*, 365−374.
(48) Cao, Y. *Synth. Met.* **1990**, *35*, 319−332.

ACKNOWLEDGMENT

Ormecon GmbH and especially Dr. Jörg Posdorfer are gratefully acknowledged for the PANI water dispersion samples (including D1012W-1), which made it possible to initiate this project. Mr. Sten Lindholm is also acknowledged for his kind assistance concerning practical aspects of the SIA instrument. This work is part of the activities of the Åbo Akademi Process Chemistry Centre within the Finnish Centre of Excellence Program (2000-2011) sponsored by the Academy of Finland.

SUPPORTING INFORMATION AVAILABLE

Derivation of the equation for determination of the protonation constant of the water dispersion of polyaniline nanoparticles, This material is available free of charge via the Internet at http://pubs.acs.org.

Received for review December 20, 2005. Accepted March 6, 2006.

AC052252U